AGU PUBLICATIONS

JGR

Journal of Geophysical Research: Atmospheres

RESEARCH ARTICLE

10.1002/2016JD025532

Key Points:
- Space observations of lightning are used to explore the global distribution of continuing current
- 11.2% of lightning flashes detected from space contain continuing current
- Oceanic and winter lightning are more likely to contain continuing current

Supporting Information:
- Supporting Information S1

Correspondence to:
P. M. Bitzer,
pm.bitzer@uah.edu

Citation:
Bitzer, P. M. (2017), Global distribution and properties of continuing current in lightning, *J. Geophys. Res. Atmos.*, *122*, 1033–1041, doi:10.1002/2016JD025532.

Received 17 JUN 2016
Accepted 21 NOV 2016
Accepted article online 23 NOV 2016
Published online 18 JAN 2017

Global distribution and properties of continuing current in lightning

Phillip M. Bitzer[1]

[1] Department of Atmospheric Science, University of Alabama in Huntsville, Huntsville, Alabama, USA

Abstract Continuing current is a process in lightning in which the current in a conducting channel can flow for much longer than in a typical lightning discharge. The phenomenon can be characterized by the continuous optical emission that accompanies the current flow. Using the Lightning Imaging Sensor (LIS), lightning with continuing current is identified on a global scale. Lightning that contains optical emission over at least five consecutive LIS frames, roughly 7–9 ms, are classified as continuing current flashes. This differs from typical lightning discharges that produce optical emission for one or two consecutive frames. Of the flashes detected by LIS, 11.2% contain continuing current. These flashes optically radiate over a larger footprint and have a longer duration than ones that do not. The spatial distribution of these flashes indicates that regions of high lightning activity may not be correlated with a high likelihood of continuing current flashes. Further, oceanic and winter lightning are shown to have a higher proportion of continuing current flashes. Finally, 25–40% of flashes identified by LIS to have continuing current have only an intracloud pulse detected by the National Lightning Detection Network (NLDN), with no cloud-to-ground strokes detected.

1. Introduction

While most lightning flashes contain discrete large-scale discharges in which current flows for a few hundred microseconds, there is a class of lightning in which the current flows for hundreds of milliseconds. This process is referred to as continuing current [e.g., *Brook et al.*, 1962; *Kitagawa et al.*, 1962]. These discharges produce continuous optical emission associated with the long current flow. Further, these flashes generally neutralize more charge than a typical lightning flash. In addition to the increased risk of damage due to the long lasting current and large charge transfers, this flash type has been associated with various phenomena, including sprites [*Bell et al.*, 1998; *Cummer and Füllekrug*, 2001] and the initiation of forest fires [*Latham and Williams*, 2001, and references therein].

Observations of lightning discharges often use the optical emission to identify continuing current [e.g., *Ballarotti et al.*, 2005; *Saba et al.*, 2006; *Biagi et al.*, 2007]. However, the long lasting current also results in relatively large and long electrostatic changes. While the electrostatic change associated with a typical cloud-to-ground (CG) stroke is on the order of a millisecond [*Krehbiel*, 1981], the electrostatic change for strokes with continuing current can last for hundreds of milliseconds [e.g., *Brook et al.*, 1962; *Kitagawa et al.*, 1962; *Livingston and Krider*, 1978; *Shindo and Uman*, 1989]. In addition, magnetic field measurements can be used to identify continuing current at relatively large range using the "quasi-static magnetic field" [*Ross et al.*, 2008]. This has been used to explore the large charge transfers associated with this type of discharge [*Lu et al.*, 2012; *Cummer et al.*, 2013].

Previous research into continuing current has explored its occurrence in terms of the duration of the current [*Rakov and Uman*, 2007; *Shindo and Uman*, 1989; *Saba et al.*, 2006; *Lapierre et al.*, 2014]. It has been suggested that 30–50% of negative CG flashes contained continuing current of greater than 40 ms [*Rakov and Uman*, 2007, p.112]. *Shindo and Uman* [1989] found that 33/90 (37%) negative CG flashes contain at least 10 ms of continuing current; discharges with less than 10 ms of continuing current were labeled as "ambiguous." To explore this lower bound, *Ballarotti et al.* [2005] used video measurements and found that 28% of negative CG strokes contain at least 3 ms of continuing current.

Because most continuing current investigations typically rely on nearby video and/or electric field measurements, they can be somewhat limited in the spatial domain studied. This study utilizes space-based optical

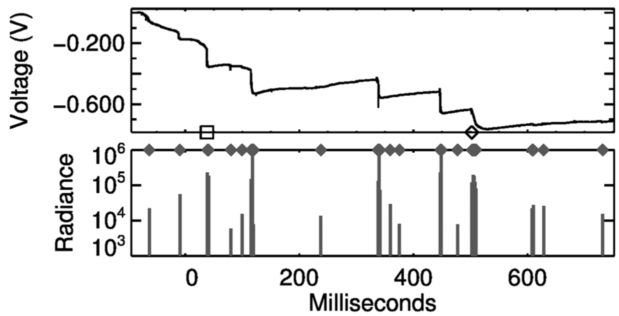

Figure 1. A nine-stroke negative cloud to ground flash that occurred on 25 June 2010. (top) The measured voltage (proportional to the electric field) waveform from a HAMMA sensor approximately 30 km from the discharge. (bottom) The LIS groups (gray diamonds and vertical bars). Each vertical gray bar has a width that corresponds to an approximate LIS frame, and the height of the bar is determined by the LIS radiance. Although LIS reports this value as "radiance" and is labeled as such here, strictly speaking it is the spectral energy density with units of μJ sr^{-1} m^{-2} μm^{-1} [*Koshak*, 2010]. Expanded views of the strokes marked with the square and diamond are presented in Figures 2 and 3, respectively. For reference, $t = 0$ corresponds to 63217.400 s past midnight (UTC).

measurements from the Lightning Imaging Sensor (LIS) over a 12 year period (2002–2013) to investigate the occurrence of continuing current in lightning flashes on a global scale. Spatial and temporal characteristics of this phenomenon are discussed. Given the impending launches of the Geostationary Lightning Mapper and the Lightning Imager, space-based optical measurements will be available in near real time; this study provides a methodology that can be used to identify this flash type from these space-based measurements.

2. Instrumentation and Methodology

2.1. Lightning Imaging Sensor

LIS was on board the Tropical Rainfall Measuring Mission satellite, which was in low Earth orbit with a 35° inclination. Fundamentally, LIS detects optical emission from lightning using a CCD pixel array. Each pixel has a footprint of approximately 4.5 km × 4.5 km, and the entire field of view is approximately 600 km × 600 km. A full description of the LIS instrument can be found in *Christian et al.* [2000], but pertinent attributes are discussed herein.

LIS detects the optical emission received in a pixel in a particular time period, referred to as a frame; the frame integration time has been found to be 1.79 ms, using on-orbit data [*Bitzer and Christian*, 2014]. During each frame, the optical emission detected in each pixel is used to determine the background [*Christian et al.*, 2000; *Koshak et al.*, 2000]. A running average of these values are then subtracted from the detected emission in the current frame. When the resulting signal exceeds a deterministic, but variable, threshold, a possible lightning event is identified. Further processing eliminates false events [*Christian et al.*, 1989].

The taxonomy of LIS lightning data is often presented in a child-parent relationship. A single pixel that contains a lightning signal is known as an LIS event. Contiguous LIS events in a single frame are classified as LIS groups. Hence, LIS events are the children of a LIS group. Groups that are coherent in time and space are called flashes; groups are the children of a LIS flash. The temporal and spatial parameters used to classify flashes are 330 ms and 5.5 km; more details can be found in *Mach et al.* [2007].

The manner in which LIS detects lightning signals allows it to identify the optical emission from lightning on top of a potentially bright background, such as a sunlit cloud, in a robust manner. However, the constantly updating background limits the ability for LIS to detect a signal such as continuing current. For example, consider a constant light source. In this scenario, every frame will effectively raise the background; eventually, the assumed background can reach a level such that the signal is below the detection threshold. Thus, LIS has a tendency to "self-quench" a continuing current signature.

2.2. Identification of Continuing Current

Lightning discharges detected by LIS, such as return strokes, K changes, and other optically bright processes, typically produce a single group [*Bitzer et al.*, 2016]. Occasionally, the light from a single discharge can be split across frames, resulting in two LIS groups [e.g., *Østgaard et al.*, 2013]. Since lightning with continuing current produces optical emission that can last for several consecutive frames, this unique signature in the LIS data can be exploited to separate continuing current discharges from those without.

As a representative example illustrating the differences in optical emission detected by LIS for various types of discharges, consider the seven-stroke negative CG flash in Figure 1 comparing the LIS optical emission and the electric field waveform recorded by a Huntsville Alabama Marx Meter Array (HAMMA) sensor [*Bitzer et al.*, 2013]. Most of the return strokes produce one or two LIS groups; there are also isolated LIS groups

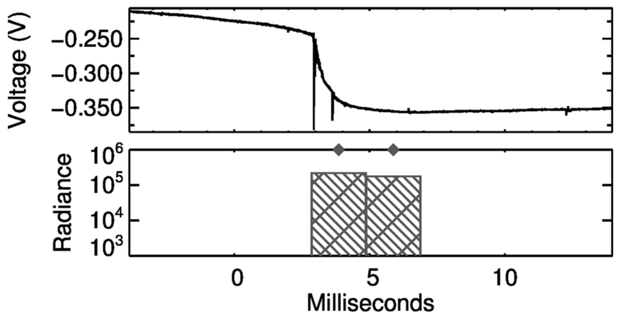

Figure 2. A negative CG return stroke with no continuing current. This stroke corresponds to the one marked with a square in Figure 1 and has a similar plot layout. Only two consecutive LIS groups were detected with this stroke. For reference, $t = 0$ corresponds to 63217.435 s past midnight (UTC).

associated with individual intracloud (IC) pulses (e.g., K changes), as determined from the electric field record. For reference, the National Lightning Detection Network (NLDN) [*Cummins and Murphy*, 2009] detected four of these strokes (not shown).

The difference in the signature of LIS optical emission can be elucidated with two strokes. Consider the stroke at $t \approx 38$ ms (marked with a square). This stroke, shown in detail in Figure 2, has two LIS groups. While it is possible the light from the return stroke has been split across frames, the electric field record contains a second return stroke signature approximately 1 ms after the main return stroke, suggesting there may be a separate connection to ground. Regardless, this stroke and most of the others in the flash are associated with one or two LIS groups, the typical LIS signature associated with a stroke. However, the last stroke in Figure 1 (at $t \approx 500$ ms, marked with a diamond) has five LIS groups. The HAMMA record is used to determine the duration of continuing current using a method similar to that of *Lapierre et al.* [2014], and the continuing current is determined to have lasted for approximately 22 ms (Figure 3). The optical emission measured by LIS in the five consecutive frames suggests the current last for approximately 7 – 9 ms, depending on when the optical emission starts relative to the frame integration times. This example also demonstrates that the duration of continuing current determined from LIS measurements should be considered a minimum. This is either due to the self-quenching nature of LIS, and/or it could reflect a reduced amount of light produced by the discharge such that it falls below the LIS detection threshold.

In order to identify the signature of continuing current using LIS, we begin with the flash data. We then identify the child groups of each flash. The use of flash data ensures the radiance-weighted locations of the groups associated with each flash are near each other, as defined by the spatial parameter in the flash sorting algorithm. If optical emission is detected in at least five consecutive frames, which manifests as five groups in consecutive frames, i.e., time contiguous groups, then the flash is considered to have continuing current. The methodology to determine if groups fall in consecutive frames is similar to that of *Bitzer and Christian* [2014]. Using the LIS frame integration time of 1.79 ms, the signature of five consecutive groups suggests a discharge with at least 7 – 9 ms of continuous optical emission.

Since LIS can detect individual discharges from an intracloud leader in as many as four consecutive frames [*Brunner*, 2016], this study uses a minimum of five consecutive frames to characterize continuing current. This minimizes the possibility that the data set contains noncontinuing current events; however, this methodology will not identify discharges with very short continuing current. In addition, the manner in which LIS detects optical emission implies the flashes analyzed herein likely have longer duration continuing current than that are directly measured by LIS. Hence, the classification of continuing current flashes into very short, short, and long used in previous research is not used [e.g., *Saba et al.*, 2006; *Lapierre et al.*, 2014]. Finally, there may be sequences of lightning discharges that produce optical emission in five or more consecutive frames that are not associated with continuing current, e.g., long IC

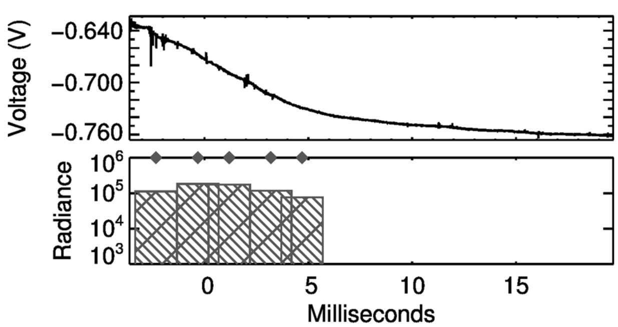

Figure 3. A negative CG return stroke with continuing current. This stroke corresponds to the one marked with a diamond in Figure 1 and has a similar plot layout. There are five consecutive LIS groups that were detected with this stroke, a manifestation of the continuing current. For reference, $t = 0$ corresponds to 63217.905 s past midnight (UTC).

Table 1. Flashes With Continuing Current as a Function of the Number of Time Contiguous Groups[a]

Contiguous Groups	5	6–7	8–10	11–20	>20
Approx. duration (ms)	7–9	9–13	13–18	18–40	>40
Number	612,258	640,992	374,817	258,255	33,523
Percent of continuing current	31.89	33.39	19.52	13.45	1.75
Percent of total flashes	3.57	3.74	2.19	1.51	0.20

[a]See the supporting information for the full distribution.

leaders with many discrete IC pulses capable of producing optical emission detectable from space. These are likely rare and have a minimal impact on the results herein.

In this study, we use LIS data to detect the occurrence of continuing current on a global basis. The signature of at least five time contiguous groups in LIS flashes is identified for the 12 year period of this study. Because LIS is in low Earth orbit, an estimate of the global occurrence of these flash types can be found. Further, the spatial distribution of these flashes can be studied, in particular the distribution of continuing current flashes over the ocean and land. In addition, diurnal and seasonal variations in the distribution are investigated. Since LIS does not discriminate between cloud-to-ground and intracloud flashes, all LIS-detected flashes are considered in this study. However, the data set is supplemented with data from a ground-based lightning network to further classify these flashes.

3. Results

3.1. Global Characteristics

LIS detected 1,919,845 flashes with continuing current for the years 2002–2013; 11.2% of LIS-detected flashes contain continuing current of at least 7 ms (Table 1). Further, 7.6% have more than 9 ms of continuing current. Again, this should be considered a lower bound due to the method in which LIS detects lightning. The yearly frequency of occurrence of continuing current flashes is essentially flat over the 12 year period (not shown).

Flashes in which a continuing current signature (at least five time contiguous groups) occurs are binned into 1° × 1° bins (Figure 4). Several hot spots of flashes with continuing current occur globally, notably regions off the eastern coast of North America, the northern part of South America into Central America, in central Africa, and over Indonesia exhibit a large number of flashes with continuing current. Notably, the hot spot off the eastern coast of North America coincides with a relative maxima in lightning detected by long range

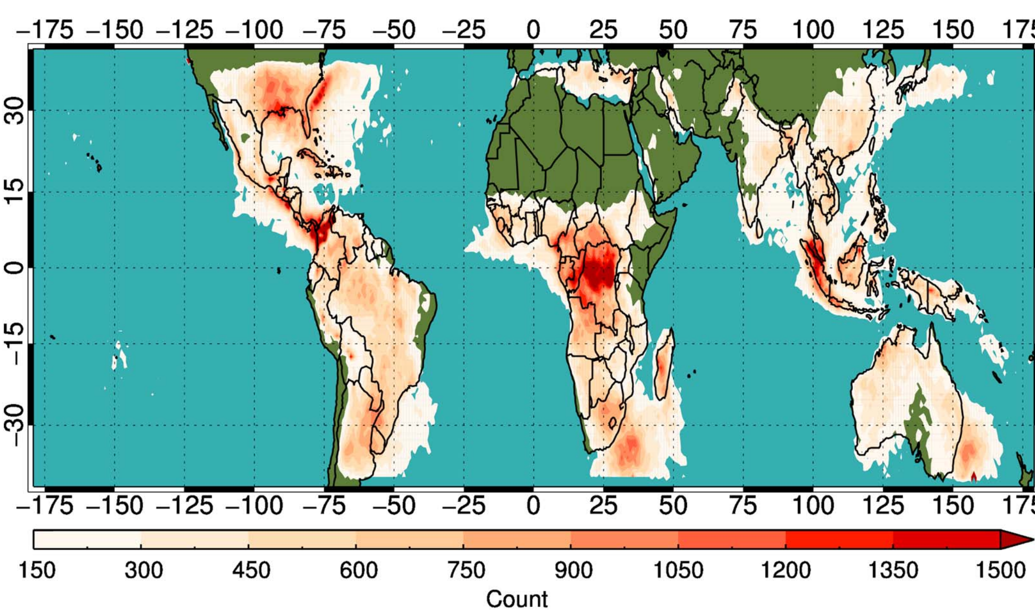

Figure 4. Global distribution of flashes with continuing current. Bins with less than 150 continuing current flashes in the 12 year period are not shown. Most of these bins fall in oceanic areas.

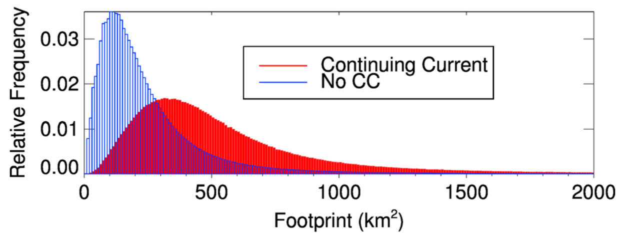

Figure 5. LIS derived footprint of flashes. The median of flash size for a flash with continuing current is 450 km^2, while the median size is 184 km^2 for flashes without continuing current.

ground-based networks [*Holle*, 2013; *Virts et al.*, 2015]. Secondary hot spots exist off the eastern coast of southern Africa, the eastern coast of southern Australia, and in the central United States. As with the total number of continuing current flashes, these hot spots are relatively stable over the 12 year period (not shown).

Figure 4 is not the raw count of flashes detected by LIS with continuing current. It has been scaled to account for the view time of LIS. Generally speaking, LIS views regions near the equator for less time than the higher latitudes [*Cecil et al.*, 2012], and this has been accounted for in Figure 4. The raw count of flashes with continuing current is available in the supporting information.

The footprint of the optical emission of flashes is provided with the LIS data [*Boccippio et al.*, 2000]. On average, continuing current flashes have a larger optical footprint than ones that do not (Figure 5). Flashes with continuing current have a mean footprint of 573 km^2 (standard deviation 464 km^2), while flashes without continuing current have a mean footprint of 255 km^2 (standard deviation 265 km^2).

In addition, flashes with continuing current generally have a longer duration than ones that do not. The nearly two million flashes that contain continuing current have a mean duration of 440 ms (median 392 ms) with a standard deviation of 320 ms. By contrast, the 15.2 million flashes without continuing current detected by LIS have a mean duration of 231 ms (median 193 ms) with a standard deviation of 211 ms.

Besides differences in the size and duration, the relative frequency in which flashes with continuing current occur varies spatially. Figure 6 shows the ratio of flashes with continuing current to all flashes detected by LIS in each bin. While oceanic flashes are less frequent than continental flashes [*Christian and Latham*, 1998; *Cecil et al.*, 2012], oceanic flashes are more likely to contain continuing current than continental flashes. Quantitatively, 42.5% of the flashes with continuing current occur over oceanic areas, while only 20.2% of the flashes that do not have continuing current occur over oceanic areas. The percentage of flashes that contain continuing current over land rarely exceeds 20% in any 1 × 1° bin.

Further, Figure 6 illustrates differences between the global climatology of all lightning, including the tropical "chimneys" [e.g., *Williams and Sátori*, 2004] and the occurrence of continuing current. Lightning frequently

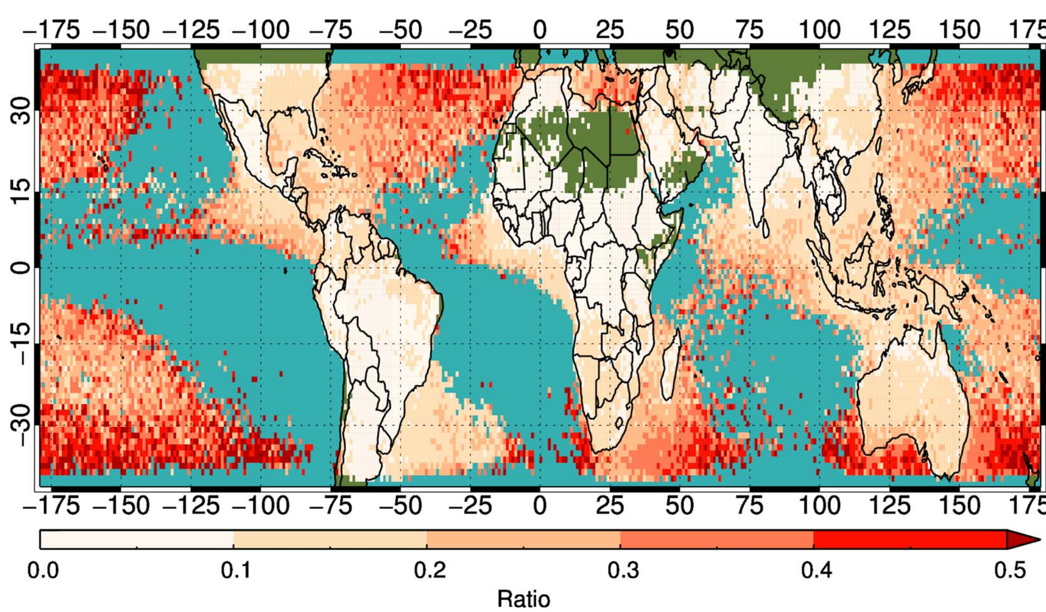

Figure 6. The ratio of flashes with continuing current to all flashes detected by LIS. Bins with less than 10 total flashes are not shown.

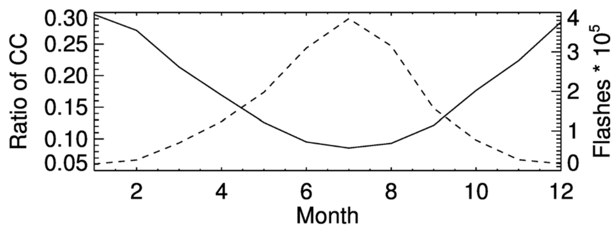

Figure 7. Annual variation of the ratio of flashes with continuing current and without (dashed line) near North America.

occurs in the Congo in Africa, near the northern coast of South America, along the Himalayan Mountains in India, and in the state of Florida in the United States [e.g., Figure 2 of *Cecil et al.*, 2012]. Yet in each of these regions the percentage of flashes with continuing current is relatively low.

3.2. Temporal Characteristics

To explore the seasonal relationship between the frequency of flashes and the likelihood of continuing current, consider flashes in the data set that occur near North America in a domain of latitude between 20° and 35°, and longitude between −130° and −70°. As expected, lightning frequency peaks during the North American summer (Figure 7). However, the monthly percentage of flashes with continuing current peaks during the winter when lightning frequency is relatively low. Hence, the occurrence of continuing current is anticorrelated with the frequency of all flashes. As is the case spatially, periods with less frequent lightning exhibit a higher percentage of continuing current.

Overall, the detection efficiency of LIS varies from 70% at noon local time to 90% during the night [*Cecil et al.*, 2012]. This is due to the increased ability to detect the lightning optical emission relative to a darker background at night [*Boccippio et al.*, 2002; *Christian et al.*, 2003]. Generally speaking, this could lead to a more robust detection of the continuing current signature at night since the lightning signal is much greater than the background. Hence, there would be an increase in the number of frames for the assumed background to increase to a level that quenches a lightning signal. This is possibly reflected in the plot of the number of continuing current flashes as a function of local hour (Figure 8). In this figure, the phase of the peak of flashes with and without continuing current is largely the same. However, the peak occurs in late afternoon for the noncontinuing current distribution and is much larger than the overnight peak. Conversely, the overnight peak of the continuing current distribution is larger than the daytime peak. This suggests that lightning during the overnight hours is more likely to contain continuing current than during the day. However, caution should be taken with this result. This observation could be due to instrumental effects, or it may reflect inherent differences in nighttime storms that may lead to continuing current. More detailed work with supporting ground-based measurements is needed to fully understand the underlying cause, as might be afforded by time-continuous space-based optical observations such as those by GLM.

3.3. Flash Type

Since optical measurements are unable to identify individual flashes as intracloud or cloud to ground, NLDN data are used to further explore the flashes that have continuing current as a function of flash type. Specifically, the data set is restricted to the years 2008–2013, and flashes identified with continuing current near North America are used to maximize NLDN detection efficiency. While the detection efficiency of CG strokes (60–80%) and CG flashes (90–95%) is higher than that of IC flashes (18–34%, unknown for IC pulses) [*Cummins and Murphy*, 2009, and references therein], NLDN is an ideal system to classify the LIS flash type. For each flash with continuing current, NLDN strokes/pulses within 330ms and 0.25° latitude and longitude are identified. The choice of the temporal and spatial constraints used to assign a flash type to a LIS flash is robust over a range of constraints and only affects the results by a few percentage points. Results from selected

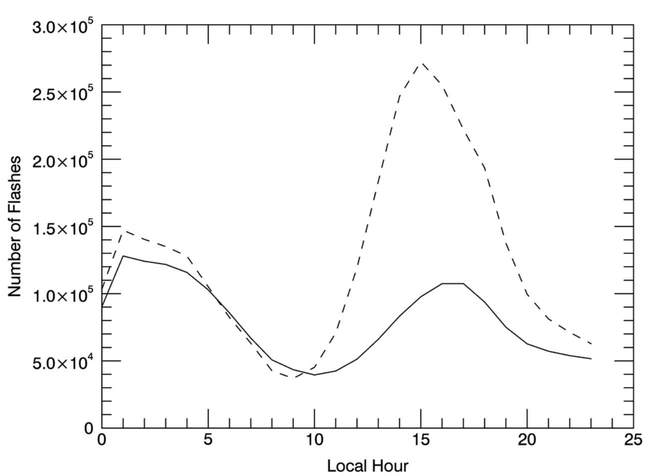

Figure 8. The number of flashes detected by LIS with continuing current (solid) and without (dashed) as a function of local hour. The number of flashes without continuing current has been scaled down by a factor of 5.

choices of the constraints are outlined in the supporting information. If only one stroke is found, then the classification and peak current of that stroke are used to classify the flash. If any CG strokes are within the limits, the stroke with the largest absolute magnitude peak current is used. If multiple IC pulses are within the limits but no CG strokes are detected, the first IC pulse is used.

There were 130,126 flashes identified with the signature of continuing current by LIS in the domain of this part of the analysis. NLDN detected at least one stroke/pulse in 55,743 (56.0%) in these flashes. Of the flashes detected by NLDN, 42,553 (76.3%) had at least one cloud-to-ground stroke. Roughly half, 23,471 (55.2%), of the flashes with a cloud-to-ground stroke were positive, using the classification scheme outlined.

However, the NLDN classification for small positive peak current strokes can be misclassified [*Cummins and Murphy*, 2009, and references therein]. To explore this impact on the results, the analysis is repeated by assuming any stroke with a peak current in the range 0–15 kA is assumed to be intracloud. Further, any strokes with a peak current greater than 15 kA is assumed to be cloud to ground. With this assumption, the number of flashes classified as cloud to ground is reduced to 31,927 (57.3%). Of these, 12,845 (40.2%) are classified as positive CGs.

4. Discussion and Conclusions

Of all the flashes detected by LIS, 11.2% contain continuing current. Several regions in which continuing current flashes occur frequently are colocated with peaks in lightning activity. However, there are differences in the location of active regions of all lightning and regions in which relatively high fractions of continuing current flashes occur. Notably, northern India is a region in which lightning activity is a relative maximum [*Cecil et al.*, 2012, Figure 2]; however, this region has a relatively low count of continuing current flashes. In the continental United States, Florida has a large number of flashes, while the peak for flashes with continuing current is located over Louisiana and off the eastern coast. Regions off the southern coast of Africa and Australia also exhibit offsets between the peak in all lightning activity and continuing current flashes. Clearly, storm dynamics that produce a lot of lightning may not necessarily also produce a large number of continuing current flashes.

Oceanic and winter lightning are less frequent [e.g., *Cecil et al.*, 2012] but are more likely to contain continuing current. These storms typically have weaker updrafts, which suggest the likelihood that storms that have this characteristic are more likely to produce flashes with continuing current. The weaker updrafts suggest that charging rates are smaller, allowing for larger charge regions to develop before lightning is initiated. This in turn provides a larger charge region available to be neutralized by a flash. More work remains to be done for a more definitive conclusion, however. A target study utilizing electric field change data, optical measurements, and radar could provide support for this hypothesis.

It has been hypothesized that continuing current flashes neutralize charge in regions of the thunderstorm that extend out in space from the initial charge source region [*Krehbiel et al.*, 1979; *Saba et al.*, 2006]. Further, flashes with continuing current are "associated with the tapping of fresh charge regions in the cloud" [*Rakov and Uman*, 2007, p.176]. The analysis herein using optical emission shows that continuing current flashes typically have a larger optical footprint, suggesting the optical footprint of a flash is related to the volume of charge neutralized in a flash. In addition, since continuing current flashes neutralize more charge on average, the relationship between storm dynamics and lightning may differ when these flashes occur. This may affect research that uses lightning data as a proxy for storm intensification [e.g., *Schultz et al.*, 2009]. Although continuing current flashes are more likely to occur during times in which the flash rate is lower, these can neutralize more charge on average and contribute differently to the overall electrical energy budget of a storm.

Depending on the classification parameters of the ground-based system, approximately 60–75% of flashes that LIS observed to contain continuing current also have a cloud-to-ground stroke. Of these, approximately 40–55% of these are positive CGs. Further, there are a nontrivial number of flashes with five or more contiguous groups that do not have a cloud-to-ground stroke but only have an intracloud pulse. Though possible some of these are could be due to misclassification, these results suggest there are intracloud flashes with continuous optical emission, implying continuing current. This has been rarely reported in the literature [e.g., *Proctor*, 1983]. While continuing current flashes are usually discussed in the context of CG flashes, the analysis herein shows that there are flashes with continuing current that do not have a detected cloud-to-ground stroke but only have an IC pulse detected. More work needs to be done to further support this result. A ground-based system capable of detecting electrostatic changes such as HAMMA [*Bitzer et al.*, 2013] or the Langmuir Electric Field Array [*Sonnenfeld and Hager*, 2013] would be ideally suited for this.

This work has important applications to future space-based instruments using optical emission to detect lightning. The Geostationary Lightning Mapper (GLM) is currently scheduled for launch in November 2016 and will operate in a similar manner as LIS [*Christian et al.*, 1989; *Goodman et al.*, 2014]. This will provide hemispheric, continual monitoring of lightning activity and possible continuing current. In addition, a flight spare of LIS is scheduled to be launched in November 2016 to be deployed on the International Space Station (ISS). The ISS-LIS will provide lightning measurements in the same manner as LIS, providing a bridge by which researchers can directly compare LIS science results to GLM. In addition, European Meteosat Third Generation Lightning Imager (LI) is scheduled for launch on 2021 [*Dobber and Kox*, 2016]. This will enable opportunities to explore geostationary observations of lightning over Europe and Africa. In addition, the frame rate for LI is designed to be 1 ms, shorter than LIS and GLM, which will provide a finer time resolution of the optical emission to further refine the methodology introduced herein.

The most immediate impact of the identification of continuing current flashes, particularly with geostationary instruments such as GLM, is the relationship with lightning-initiated forest fires. Since continuing current flashes have been associated with forest fires [*Fuquay et al.*, 1967], instruments that can observe this type of lightning over a large domain will be helpful for early identification of the initiation of these events.

In addition, sprite production is often associated with continuing current flashes [e.g., *Cummer and Füllekrug*, 2001; *Rycroft and Odzimek*, 2010]. The analysis herein shows that continuing current flashes often occur off the eastern coast of North America. This is also a region in which sprites are often detected [*Cummer et al.*, 2013]. The identification of other continuing current hot spots may be leveraged to focus sprite observation studies. In addition, GLM will provide identification of continuing current flashes on a time-continuous basis and at higher latitudes, allowing more robust comparisons between sprites and continuing current flashes.

Acknowledgments

This study was partially supported by NOAA grant Z7813005 (Cooperative Institute for Climate and Satellites-CICS) at the University of Maryland/ESSIC as part of the GOES-R Risk Reduction Research and NASA grant NNM05AA22A. The author thanks Jeff Burchfield, Hugh Christian, and Rich Blakeslee for providing valuable insight and comments on the manuscript. The Lightning Imaging Sensor (LIS) Science Data were obtained from the NASA EOSDIS Global Hydrology Resource Center (GHRC) DAAC, Huntsville, Alabama. These data are available, consistent with AGU data policy. HAMMA data are available from the author. NLDN data provided to the NASA Lightning Imaging Sensor (LIS) instrument team and the NASA LIS Data Center via the NASA EOSDIS Global Hydrology Resource Center (GHRC) DAAC located at the Global Hydrology and Climate Center (GHCC), Huntsville, Alabama, through a license agreement with the Vaisala Group. The data available from the NASA EOSDIS GHRC DAAC are restricted to collaborators that have a working relationship with the NASA Marshall Space Flight Center (MSFC) Lightning Group.

References

Ballarotti, M. G., M. M. F. Saba, and O. Pinto (2005), High-speed camera observations of negative ground flashes on a millisecond-scale, *Geophys. Res. Lett.*, *32*, L23802, doi:10.1029/2005GL023889.

Bell, T. F., S. C. Reising, and U. S. Inan (1998), Intense continuing currents following positive cloud-to-ground lightning associated with red sprites, *Geophys. Res. Lett.*, *25*(8), 1285–1288.

Biagi, C., K. Cummins, K. Kehoe, and E. Krider (2007), National Lightning Detection Network (NLDN) performance in southern Arizona, Texas, and Oklahoma in 2003–2004, *J. Geophys. Res.*, *112*, D05208, doi:10.1029/2006JD007341.

Bitzer, P. M., and H. J. Christian (2014), Timing uncertainty of the lightning imaging sensor, *J. Atmos. Oceanic Technol.*, *32*(3), 453–460, doi:10.1175/JTECH-D-13-00177.1.

Bitzer, P. M., H. J. Christian, M. Stewart, J. Burchfield, S. Podgorny, D. Corredor, J. Hall, E. Kuznetsov, and V. Franklin (2013), Characterization and applications of VLF/LF source locations from lightning using the Huntsville Alabama Marx Meter Array, *J. Geophys. Res. Atmos.*, *118*, 3120–3138, doi:10.1002/jgrd.50271.

Bitzer, P. M., J. C. Burchfield, and H. J. Christian (2016), A Bayesian approach to assess the performance of lightning detection systems, *J. Atmos. Oceanic Technol.*, *33*(3), 563–578, doi:10.1175/JTECH-D-15-0032.1.

Boccippio, D., W. Koshak, and R. Blakeslee (2002), Performance assessment of the optical transient detector and lightning imaging sensor. I- Predicted diurnal variability, *J. Atmos. Oceanic Technol.*, *19*(9), 1318–1332.

Boccippio, D. J., S. J. Goodman, and S. Heckman (2000), Regional differences in tropical lightning distributions, *J. Appl. Meteorol.*, *39*(12), 2231–2248, doi:10.1175/1520-0450(2001)040<2231:RDITLD>2.0.CO;2.

Brook, M., N. Kitagawa, and E. J. Workman (1962), Quantitative study of strokes and continuing currents in lightning discharges to ground, *J. Geophys. Res.*, *67*(2), 649–659, doi:10.1029/JZ067i002p00649.

Brunner, K. (2016), Explorations in intracloud lightning and leader processes, Master's thesis, University of Alabama in Huntsville, Huntsville, Ala.

Cecil, D. J., D. E. Buechler, and R. J. Blakeslee (2012), Gridded lightning climatology from TRMM-LIS and OTD: Dataset description, *Atmos. Res.*, *135*, 404–414, doi:10.1016/j.atmosres.2012.06.028.

Christian, H., R. Blakeslee, and S. Goodman (1989), The detection of lightning from geostationary orbit, *J. Geophys. Res.*, *94*(D11), 13,329–13,337.

Christian, H., et al. (2003), Global frequency and distribution of lightning as observed from space by the Optical Transient Detector, *J. Geophys. Res.*, *108*(D1), 4005, doi:10.1029/2002JD002347.

Christian, H. J., and J. Latham (1998), Satellite measurements of global lightning, *Q. J. R. Meteorol. Soc.*, *124*(549), 1771–1773, doi:10.1002/qj.49712454919.

Christian, H. J., R. J. Blakeslee, S. J. Goodman, and D. Mach (2000), Algorithm Theoretical Basis Document (ATBD) for the Lightning Imaging Sensor (LIS), *Tech. Rep.*, NASA/Marshall Space Flight Center, Alabama. [Available at http://eospso.gsfc.nasa.gov/sites/default/files/atbd/atbd-lis-01.pdf.]

Cummer, S. A., and M. Füllekrug (2001), Unusually intense continuing current in lightning produces delayed mesospheric breakdown, *Geophysical Res. Lett.*, *28*(3), 495–498, doi:10.1029/2000GL012214.

Cummer, S. A., W. A. Lyons, and M. A. Stanley (2013), Three years of lightning impulse charge moment change measurements in the United States, *J. Geophys. Res. Atmos.*, *118*, 5176–5189, doi:10.1002/jgrd.50442.

Cummins, K., and M. Murphy (2009), An overview of lightning locating systems: History, techniques, and data uses, with an in-depth look at the US NLDN, *IEEE Trans. Electromagn. Compat.*, *51*(3), 499–518.

Dobber, M., and S. Kox (2016), Meteosat Third Generation (MTG) Lightning Imager (LI) calibration and 0-1b data processing, paper presented at 25th CALCON Technical Meeting.

Fuquay, D. M., R. G. Baughman, A. R. Taylor, and R. G. Hawe (1967), Characteristics of seven lightning discharges that caused forest fires, *J. Geophys. Res.*, *72*(24), 6371–6373, doi:10.1029/JZ072i024p06371.

Goodman, S. J., et al. (2014), World Weather Open Sci. Conf., World Meteorol. Organiz.

Holle, R. L. (2013), Diurnal variations of NLDN-reported cloud-to-ground lightning in the United States, *Mon. Weather Rev.*, *142*(3), 1037–1052, doi:10.1175/MWR-D-13-00121.1.

Kitagawa, N., M. Brook, and E. J. Workman (1962), Continuing currents in cloud-to-ground lightning discharges, *J. Geophys Res.*, *67*(2), 637–647, doi:10.1029/JZ067i002p00637.

Koshak, W. J. (2010), Optical characteristics of OTD flashes and the implications for flash-type discrimination, *J. Atmos. Oceanic Technol.*, *27*(11), 1822–1838, doi:10.1175/2010JTECHA1405.1.

Koshak, W. J., M. F. Stewart, H. J. Christian, J. W. Bergstrom, J. M. Hall, and R. J. Solakiewicz (2000), Laboratory calibration of the Optical Transient Detector and the Lightning Imaging Sensor, *J. Atmos. Oceanic Technol.*, *17*(7), 905–915, doi:10.1175/1520-0426(2000)017<0905:LCOTOT>2.0.CO;2.

Krehbiel, P. (1981), An analysis of the electric field change produced by lightning, PhD thesis, University of Manchester Inst.of Sci. and Technol., Manchester, England.

Krehbiel, P., M. Brook, and R. McCrory (1979), An analysis of the charge structure of lightning discharges to ground, *J. Geophys. Res.*, *84*(C5), 2432–2456.

Lapierre, J. L., R. G. Sonnenfeld, H. E. Edens, and M. Stock (2014), On the relationship between continuing current and positive leader growth, *J. Geophys. Res. Atmos.*, *119*, 12,479–12,488, doi:10.1002/2014JD022080.

Latham, D., and E. Williams (2001), Chapter 11: Lightning and forest fires, in *Forest Fires*, edited by E. A. Johnson and K. Miyanishi, pp. 375–418, Acad. Press, San Diego, Calif.

Livingston, J. M., and E. P. Krider (1978), Electric fields produced by Florida thunderstorms, *J. Geophys. Res.*, *83*(C1), 385–401, doi:10.1029/JC083iC01p00385.

Lu, G., S. A. Cummer, R. J. Blakeslee, S. Weiss, and W. H. Beasley (2012), Lightning morphology and impulse charge moment change of high peak current negative strokes, *J. Geophys. Res.*, *117*, D04212, doi:10.1029/2011JD016890.

Mach, D., H. Christian, R. Blakeslee, D. Boccippio, S. Goodman, and W. Boeck (2007), Performance assessment of the optical transient detector and lightning imaging sensor, *J. Geophys. Res.*, *112*, D09210, doi:10.1029/2006JD007787.

Østgaard, N., T. Gjesteland, B. E. Carlson, A. B. Collier, S. Cummer, G. Lu, and H. J. Christian (2013), Simultaneous observations of optical lightning and terrestrial gamma ray flash from space, *Geophys. Res. Lett.*, *40*, 2423–2426, doi:10.1002/grl.50466.

Proctor, D. E. (1983), Lightning and precipitation in a small multicellular thunderstorm, *J. Geophys. Res.*, *88*(C9), 5421–5440, doi:10.1029/JC088iC09p05421.

Rakov, V., and M. Uman (2007), *Lightning: Physics and Effects*, Cambridge Univ. Press, New York.

Ross, M., S. A. Cummer, T. K. Nielsen, and Y. Zhang (2008), Simultaneous remote electric and magnetic field measurements of lightning continuing currents, *J. Geophys. Res.*, *113*, D20125, doi:10.1029/2008JD010294.

Rycroft, M. J., and A. Odzimek (2010), Effects of lightning and sprites on the ionospheric potential, and threshold effects on sprite initiation, obtained using an analog model of the global atmospheric electric circuit, *J. Geophys. Res.*, *115*, A00E37, doi:10.1029/2009JA014758.

Saba, M. M. F., O. Pinto, and M. G. Ballarotti (2006), Relation between lightning return stroke peak current and following continuing current, *Geophys. Res. Lett.*, *33*, L23807, doi:10.1029/2006GL027455.

Schultz, C., W. Petersen, and L. Carey (2009), Preliminary development and evaluation of lightning jump algorithms for the real-time detection of severe weather, *J. Appl. Meteorol. Climatol.*, *48*(12), 2543–2563.

Shindo, T., and M. A. Uman (1989), Continuing current in negative cloud-to-ground lightning, *J. Geophys. Res.*, *94*(D4), 5189–5198, doi:10.1029/JD094iD04p05189.

Sonnenfeld, R. G., and W. W. Hager (2013), Electric field reversal in sprite electric field signature, *Mon. Weather Rev.*, *141*(5), 1731–1735, doi:10.1175/MWR-D-12-00220.1.

Virts, K. S., J. M. Wallace, M. L. Hutchins, and R. H. Holzworth (2015), Diurnal and seasonal lightning variability over the Gulf Stream and the Gulf of Mexico, *J. Atmos. Sci.*, *72*(7), 2657–2665, doi:10.1175/JAS-D-14-0233.1.

Williams, E., and G. Sátori (2004), Lightning, thermodynamic and hydrological comparison of the two tropical continental chimneys, *J. Atmos. Sol. Terr. Phys.*, *66*(13–14), 1213–1231, doi:10.1016/j.jastp.2004.05.015.